



Krishnamurthy, B. and Bylya, O. and Davey, K. (2017) Physical modelling for metal forming processes. Procedia Engineering. ISSN 1877-7058 (In Press) ,

This version is available at <https://strathprints.strath.ac.uk/60896/>

Strathprints is designed to allow users to access the research output of the University of Strathclyde. Unless otherwise explicitly stated on the manuscript, Copyright © and Moral Rights for the papers on this site are retained by the individual authors and/or other copyright owners. Please check the manuscript for details of any other licences that may have been applied. You may not engage in further distribution of the material for any profitmaking activities or any commercial gain. You may freely distribute both the url (<https://strathprints.strath.ac.uk/>) and the content of this paper for research or private study, educational, or not-for-profit purposes without prior permission or charge.

Any correspondence concerning this service should be sent to the Strathprints administrator: strathprints@strath.ac.uk

The Strathprints institutional repository (<https://strathprints.strath.ac.uk>) is a digital archive of University of Strathclyde research outputs. It has been developed to disseminate open access research outputs, expose data about those outputs, and enable the management and persistent access to Strathclyde's intellectual output.



International Conference on the Technology of Plasticity, ICTP 2017, 17-22 September 2017,
Cambridge, United Kingdom

Physical modelling for metal forming processes

B. Krishnamurthy^a, O. Bylya^a, K. Davey^{a,b*}

^aAdvanced Forming Research Centre, University of Strathclyde, 85 Inchinnan Drive, Inchinnan PA49LJ, UK.

^bSchool of Mechanical, Aerospace and Civil Engineering, The University of Manchester, Manchester M13 9PL, UK.

Abstract

Physical modelling has a long established history for the investigation of metal forming and other manufacturing processes. In recent times however its place and importance has diminished somewhat as a direct consequence of advances made in numerical modelling techniques. This paper re-examines the place of physical modelling and by means of selected examples demonstrates the benefits of the approach. Physical modelling often provides an indirect representation of the physics under consideration and may often involve scaling and the use of cheaper substitute materials. A question posed that has in some respects contributed to the diminution of physical modelling is whether the physical model is representative of the physics involved. Related to this question is a new approach to scaled experimentation that has appeared in the recent literature. The new approach is founded on the scaling of space itself and although the idea that space expands and distorts is not new to physics (e.g. cosmology and general relativity) its application to physical modelling is considered completely novel. The scaling concept enables the physics of processes to be projected into a scaled space and vice versa, thus providing quantification of the validity of any physical model. This aspect fortifies a particular weakness in the physical modelling approach making its reappraisal particularly timely. Selected numerical and experimental trials are being designed to showcase and reveal the benefits, validity and renewed importance of physical modelling.

© 2017 The Authors. Published by Elsevier Ltd.

Peer-review under responsibility of the scientific committee of the International Conference on the Technology of Plasticity.

Keywords: Metal forming; physical modelling; scaled experimentation; finite similitude.

* Corresponding author. Tel.: +44-0161-306-3834

E-mail address: keith.davey@manchester.ac.uk

1. Introduction

A comment attributed to Albert Einstein is that a model should be as simple as possible, but not simpler. The essence of this statement is that models are invariably approximations of real physics but not all approximations are sufficient. A sufficient model is that model which achieves its intended purpose and yet takes its simplest form.

In this paper a distinction is drawn between empirical, mathematical, computational and physical models. Empirical models have no real predictive power and can best be considered to be an accumulation of experimental knowledge although possibly succinctly captured by mathematical expressions. The absence of underpinning physical laws is the principal facet of an empirical model. A mathematical model on the other hand is founded on physical laws but suitably simplified so that closed-form solutions can be obtained from the mathematical description, i.e. the governing equations can be solved analytically. Mathematical models have a critical role to play in teaching (for example), where reasonably simple solutions can be used to describe and investigate bits of science and engineering. On occasions a closed-form solution can be incorporated into a more sophisticated computational model to aid convergence. A particular limitation of mathematical models is that they contain modelling errors [1] arising from the physics neglected, which can be difficult to quantify. A computational model is invariably underpinned by a mathematical model but the use of computers permits the investigation of seriously complex behaviors. It is beyond contention that computational models now play an almost dominant role in the modelling of real processes. In view of this dominance it is reasonable to ask with metal forming in mind whether physical modelling has anything significant to offer. The success of computational models however and the ease in which more complicated physics can be incorporated is somewhat perversely its greatest limitation. Rather than leading to the simplest model (as Einstein remarked) this can often lead to models of extraordinary complexity involving large numbers of internal variables and parameters and quite often requiring many experiments in order to simply initialize them [2].

A physical model is restricted here to be a model that is bounded by the physical laws of the universe but is tangible, so can be touched, measured and observed. Physical modelling for the investigation of metal forming processes has a long and distinguished history [3-7] and has provided a means to perform research and analysis on complex processes. A physical model for a forging process for example would typically involve the substitution of materials (possibly both dies and billet) and possibly involve scaling to facilitate an investigation under laboratory conditions. A critical concern however, is that by changing materials and scaling there is invariably a change in process behavior. In order to minimize any such change it is clearly necessary to select substitute materials with great care. The focus of this paper is on this aspect and on a methodology that is able to quantify differences that occur with physical modelling and to enable the focus on important aspects of interest. The method considered is designed to make physical models more reliable and useful. Physical models have the key advantage that they can offer immediate results and for extraordinarily complex processes can provide these relatively cheaply and competitively in contrast to numerical methods.

All physical models in metal forming applications have focused thus far on issues surrounding the materials, processing and machinery involved along with contact conditions. Space takes center stage in the theory considered in this paper as scaling is not achieved by scaling objects within a particular space but by scaling space itself. The focus on space rather than the objects within it naturally leads to integral transport equations since these are founded on the control-volume concept. A more fitting name for “control volume” might be “control space” since the concepts involved are indubitably about space and the transfers of material, energy, entropy etc. through and across the boundaries of the space as quantified by a moving control volume. The concept of finite similitude immediately follows, which exists when observers are unable to distinguish between two similar processes being performed within the spaces identified. If observers “observe” transfers in the same proportions in and out of the two identified spaces, then the processes within the space are deemed to possess (finite) similarity. The focus on space in this way lifts the focus from the particular details on the metal forming processes to the physical laws that describes them.

In order to explain the concepts involved the paper begins by introducing the mappings underpinning control volume movement in Section 2 along with the transport equations for the physical and trial spaces. Section 3 focuses on the relationships arising out of the matching of integrands in the transport equations. In Section 4 material-selection issues and boundary conditions are examined. Results are provided in Section 5 to highlight the benefits and difficulties with the new physical-modelling approach.

2. Brief outline of scaling concepts

The underpinning concepts outlined in this paper are founded on the scaling of space and the matching of physics described in transport form. Six transport equations are pertinent to continuum mechanics in general and metal forming in particular and each is required to be satisfied in the physical and trial spaces. The trial space is taken to be the space where trials are intended to be performed, i.e. where physical modelling occurs, which is intended to represent at least in part the process of interest in the physical space.

The starting point for similitude is a mathematical theory underpinning the movement of control volumes Ω_{ps} and Ω_{ts} in the physical and trial spaces, respectively. A control volume is defined to be a continuous open domain Ω_{ps} (Ω_{ts}) whose closure contains the boundary Γ_{ps} (Γ_{ts}), which possess an outward pointing unit normal \bar{n}_{ps} (\bar{n}_{ts}). Spatial and temporal maps are assumed to exist, which take the form $d\bar{x}(\bar{s},t)$ and $d\tau = g(t)dt$ (or $dt = h(\tau)d\tau$ with $h(\tau)g(t) = 1$), where (\bar{x},τ) and (\bar{s},t) are coordinates in the trial and physical spaces, respectively. The differential map $d\bar{x}(\bar{s},t)$ gives rise to Nanson’s identities $dV_{ts} = |F|dV_{ps}$ and $d\bar{\Gamma}_{ts} = |F|d\bar{\Gamma}_{ps} \otimes F^{-1}$, where dV_{ts} is an elemental volume in Ω_{ts} , $F = (\partial\bar{x}/\partial\bar{s})$ and $d\bar{\Gamma}_{ts}$ is an oriented elemental area on Γ_{ts} . A typical transport equation in the physical space takes the form

$$\frac{D^*}{D^*t} \int_{\Omega_{ps}} \rho_{ps} \psi_{ps} dV_{ps} + \int_{\Gamma_{ps}} \rho_{ps} \psi_{ps} (\bar{v}_{ps} - \bar{v}_{ps}^*) \cdot \bar{n}_{ps} d\Gamma_{ps} = - \int_{\Gamma_{ps}} \bar{J}_{ps}^{\psi} \cdot \bar{n}_{ps} d\Gamma_{ps} + \int_{\Omega_{ps}} \rho_{ps} b_{ps}^{\psi} dV_{ps} \quad (1)$$

where ρ is density, \bar{v} is material velocity, $\bar{J}^{\psi} \cdot \bar{n}$ is a flux corresponding to the field variable ψ , b^{ψ} is a source term, D^*/D^* signifies a temporal transport derivative, which satisfies the relationship $D^* \bar{s} / D^* t = \bar{v}^*$ and consequently describes the movement of the control volume Ω_{ps} .

The six transport equations pertinent to continuum mechanics (and similitude) describing the transport of volume ($\psi = \rho^{-1}$), mass ($\psi = 1$), momentum ($\psi = \bar{v}$), movement ($\psi = \bar{u}$), energy ($\psi = u + 0.5\bar{v} \cdot \bar{v}$) and entropy ($\psi = s$); \bar{u} is displacement, u is specific internal energy, and s is specific entropy. There are, of course, identical transport equations governing the physics in the trial space represented by the generic form

$$\frac{D^*}{D^*\tau} \int_{\Omega_{ts}} \rho_{ts} \psi_{ts} dV_{ts} + \int_{\Gamma_{ts}} \rho_{ts} \psi_{ts} (\bar{v}_{ts} - \bar{v}_{ts}^*) \cdot \bar{n}_{ts} d\Gamma_{ts} = - \int_{\Gamma_{ts}} \bar{J}_{ts}^{\psi} \cdot \bar{n}_{ts} d\Gamma_{ts} + \int_{\Omega_{ts}} \rho_{ts} b_{ts}^{\psi} dV_{ts} \quad (2)$$

where the change in time progression is accommodated in the trial space by the symbol τ .

Substitution of Nanson’s identities $dV_{ts} = |F|dV_{ps}$ and $d\bar{\Gamma}_{ts} = |F|d\bar{\Gamma}_{ps} \otimes F^{-1}$ into Eq. (2) followed by multiplication $\alpha^{\psi} F^{\psi}$ (for greatest generality), where α^{ψ} is a scalar constant and F^{ψ} is a constant invertible matrix, provides

$$\begin{aligned} \frac{D^*}{D^*t} \int_{\Omega_{ps}} \alpha^{\psi} \rho_{ts} F^{\psi} \otimes \psi_{ts} |F| dV_{ps} + \int_{\Gamma_{ps}} g \alpha^{\psi} \rho_{ts} |F| F^{\psi} \otimes \psi_{ts} \otimes (F)^{-1} \otimes (\bar{v}_{ts} - \bar{v}_{ts}^*) \cdot \bar{n}_{ps} d\Gamma_{ps} = \\ - \int_{\Gamma_{ps}} g \alpha^{\psi} |F| \left(F^{\psi} \bar{J}_{ps}^{\psi} (F)^{-T} \right) \otimes \bar{n}_{ps} d\Gamma_{ps} + \int_{\Omega_{ps}} g \alpha^{\psi} \rho_{ps} F^{\psi} \otimes b_{ps}^{\psi} |F| dV_{ps} \end{aligned} \quad (3)$$

where products between tensor and vectors are assumed to take priority over inner products between vectors (i.e. “ \otimes ” supersedes “ \cdot ”). Finite similitude in continuum mechanics is thus defined to be achieved if the corresponding integrands in Eq. (3) and (1) match for the six transport equations.

3. The scaling rules and implications

The matching of the integrands in Eq. (3) and (1) give rise after some manipulation (see reference [8, 9]) to the relationships

$$\alpha^{\rho} \psi_{ps} = \alpha^{\psi} F^{-1} \otimes \psi_{ts} = \alpha^{\psi} \beta^{-1} \psi_{ts} \quad (\text{or } \alpha^{\psi} \psi_{ts}) \quad (4)$$

$$\alpha^{\rho} \rho_{ps}^{-1} \bar{J}_{ps}^{\psi} = \alpha^{\psi} g \rho_{ts}^{-1} F^{-1} \otimes \bar{J}_{ts}^{\psi} \otimes F^{-T} = \alpha^{\psi} g \rho_{ts}^{-1} \beta^{-2} \bar{J}_{ts}^{\psi} \quad (\text{or } \alpha^{\psi} g \rho_{ts}^{-1} \beta^{-1} \bar{J}_{ts}^{\psi}) \quad (5)$$

$$\alpha^\rho \mathbf{b}_{ps}^{\psi} = \mathbf{g} \alpha^{\psi} \mathbf{F}^{-1} \otimes \mathbf{b}_{ts}^{\psi} = \mathbf{g} \alpha^{\psi} \beta^{-1} \mathbf{b}_{ts}^{\psi} \left(\text{or } \mathbf{g} \alpha^{\psi} \mathbf{b}_{ts}^{\psi} \right) \quad (6)$$

where $\mathbf{F} = \beta \mathbf{I}$ for isotropic scaling (of principal interest here), and where $\mathbf{F}^{-1} \otimes$ is absent for scalar equations and the transport equation for volume provides $1 = \alpha^1 |\mathbf{F}| = \alpha^1 \beta^3$ and $\bar{\mathbf{v}}_{ts}^* = \mathbf{h} \mathbf{F} \otimes \bar{\mathbf{v}}_{ps}^* = \mathbf{h} \beta \bar{\mathbf{v}}_{ps}^*$. Similarly the transport equation for mass yields $\rho_{ts} = \alpha^\rho \rho_{ts} |\mathbf{F}| = \alpha^\rho \beta^3 \rho_{ts}$ along with the material velocity relationship $\bar{\mathbf{v}}_{ts} = \mathbf{h} \mathbf{F} \otimes \bar{\mathbf{v}}_{ps} = \mathbf{h} \beta \bar{\mathbf{v}}_{ps}$, where α^ρ is a free scaling parameter, which appears in Eq. (4) to (6). Each transport equation provides boundary conditions and in some cases restrictions on the scaling parameters and in the case of momentum the condition $\alpha^\rho \bar{\mathbf{v}}_{ps} = \alpha^v \bar{\mathbf{v}}_{ts}$ but since $\bar{\mathbf{v}}_{ts} = \mathbf{h} \beta \bar{\mathbf{v}}_{ps}$ it follows that $\alpha^v = \mathbf{g} \beta^{-1} \alpha^\rho$, i.e. the scaling of momentum is not arbitrary. The relationship $\alpha^v = \mathbf{g} \beta^{-1} \alpha^\rho$ is a consequence of the coupled physics with mass fluxes unsurprisingly impacting on momentum fluxes. Another important relationship from the momentum equation is $\alpha^\rho (\rho^{-1} \bar{\sigma})_{ps} = \alpha^v \mathbf{g} \beta^{-1} (\rho^{-1} \bar{\sigma})_{ts}$ relating the two stress tensors. Kinetic energies in the two systems are related by $0.5 \alpha^\rho \bar{\mathbf{v}}_{ps} \cdot \bar{\mathbf{v}}_{ps} = 0.5 \alpha^e \bar{\mathbf{v}}_{ts} \cdot \bar{\mathbf{v}}_{ts}$ but $\bar{\mathbf{v}}_{ts} = \mathbf{h} \beta \bar{\mathbf{v}}_{ps}$, which reveals an additional relationship between the scaling parameters, i.e. $\alpha^e = \mathbf{g}^2 \beta^{-2} \alpha^\rho = \mathbf{g} \beta^{-1} \alpha^v$. The energy equation provides the heat transfer relationship $\alpha^\rho (\rho^{-1} \bar{q})_{ps} = \alpha^e \mathbf{g} \beta^{-1} (\rho^{-1} \bar{q})_{ts}$ and the entropy equation reveals the temperature relationship $\alpha^s T_{ps} = \alpha^e T_{ts}$, where the scaling parameter α^s provides a means for scaling temperature.

4. Material selection and Boundary conditions

The scaled transport equations give rise to eight parameters, although 4 are dependent arising out of the interrelationship between volume, mass, momentum and energy. Six scalars are involved, i.e. $\{\alpha^1, \alpha^\rho, \alpha^v, \alpha^u, \alpha^e, \alpha^s\}$ along with a time scalar \mathbf{g} and the spatial scalar β . The eight parameters are not all independent with four constraining equations of the form $\alpha^1 = \beta^{-3}$, $\alpha^v = \mathbf{g} \beta^{-1} \alpha^\rho$, $\alpha^u = \alpha^\rho$, $\alpha^e = \mathbf{g} \beta^{-1} \alpha^v$. The fields are related in a relatively simple fashion by: $\rho_{ps} = \alpha^\rho \beta^3 \rho_{ts}$ (density), $\bar{\mathbf{v}}_{ts} = \mathbf{h} \beta \bar{\mathbf{v}}_{ps}$ (material velocity), $\bar{\mathbf{u}}_{ts} = \beta \bar{\mathbf{u}}_{ps}$ (displacement), $\alpha^\rho \bar{u}_{ps} = \alpha^e \bar{u}_{ts}$ (specific internal energy), $\alpha^s T_{ps} = \alpha^e T_{ts}$ (temperature) with the velocity relationship $\bar{\mathbf{v}}_{ts}^* = \mathbf{h} \beta \bar{\mathbf{v}}_{ps}^*$ synchronising control volume movement. The setting of the parameters is critical to a successful trial and it is appreciated that the theory with four free parameters provides limited flexibility for solutions in the trial space and in practice four is unlikely to be sufficient for a perfect match. It is necessary therefore to focus on important material properties and/or boundary conditions that are critical to the purpose of the trial and select materials judiciously.

4.1. Material selection

Certain material properties can be affected by scaling; dimensioned quantities are on the whole influenced but dimensionless ones are not. It is possible however to influence function-dimensionless quantities indirectly through their arguments. Important material relationships for metal forming are: $\bar{\sigma}$, $\gamma = \partial \bar{\sigma} / \partial \bar{\epsilon}$, $\zeta = \partial \bar{\sigma} / \partial \dot{\bar{\epsilon}}$, $\xi = \partial \bar{\sigma} / \partial T$ and each is assumed to be a function of $\bar{\epsilon}$, $\dot{\bar{\epsilon}}$ and T . However, since $\bar{\epsilon}_{ps} = \bar{\epsilon}_{ts}$, $\dot{\bar{\epsilon}}_{ps} = \mathbf{g} \dot{\bar{\epsilon}}_{ts}$ and $\alpha^s T_{ps} = \alpha^e T_{ts}$ it follows that $\bar{\sigma}_{ts} \propto \bar{\sigma}_{ps} \left(\bar{\epsilon}_{ts}, \mathbf{g} \dot{\bar{\epsilon}}_{ts}, \left(\alpha^e / \alpha^s \right) T_{ts} \right)$, $\gamma_{ts} \propto \gamma_{ps} \left(\bar{\epsilon}_{ts}, \mathbf{g} \dot{\bar{\epsilon}}_{ts}, \left(\alpha^e / \alpha^s \right) T_{ts} \right)$, and similarly $\zeta_{ts} \propto \zeta_{ps} \left(\bar{\epsilon}_{ts}, \mathbf{g} \dot{\bar{\epsilon}}_{ts}, \left(\alpha^e / \alpha^s \right) T_{ts} \right)$ and $\xi_{ts} \propto \left(\alpha^s / \alpha^e \right) \xi_{ps} \left(\bar{\epsilon}_{ts}, \mathbf{g} \dot{\bar{\epsilon}}_{ts}, \left(\alpha^e / \alpha^s \right) T_{ts} \right)$. Thus a certain degree of adjustment is possible through the parameters \mathbf{g} , α^s and $\alpha^e = \mathbf{g} \beta^{-1} \alpha^v$ but most crucial is the choice of material. The identity $\alpha^\rho (\rho^{-1} \bar{q})_{ps} = \alpha^e \mathbf{g} \beta^{-1} (\rho^{-1} \bar{q})_{ts}$ along with Fourier's law of heat conduction $\bar{\mathbf{q}}_{ps} = -k_{ps} \nabla_{ps} T_{ps}$ provides after some manipulation the relationship $k_{ps} = \alpha^s \mathbf{g} \beta k_{ts}$.

4.2. Boundary conditions

Three types of boundary condition are particularly important in metal forming, i.e. displacement/velocity, traction and heat transfer. The advantage of the transport approach is that relationships for boundary conditions are immediately provided with displacement and velocity obtained directly from $\bar{\mathbf{u}}_{ts} = \beta \bar{\mathbf{u}}_{ps}$ and $\bar{\mathbf{v}}_{ts} = \mathbf{h} \beta \bar{\mathbf{v}}_{ps}$ with traction obtained through $\alpha^\rho (\rho^{-1} \bar{\sigma})_{ps} \cdot \bar{\mathbf{n}}_{ps} = \alpha^v \mathbf{g} \beta^{-1} (\rho^{-1} \bar{\sigma})_{ts} \cdot \bar{\mathbf{n}}_{ts}$ and heat transfer provided by $\alpha^\rho (\rho^{-1} \bar{q})_{ps} \cdot \bar{\mathbf{n}}_{ps} = \alpha^e \mathbf{g} \beta^{-1} (\rho^{-1} \bar{q})_{ts} \cdot \bar{\mathbf{n}}_{ts}$. Note that for a convection boundary condition of the form $\bar{\mathbf{q}}_{ps} \cdot \bar{\mathbf{n}}_{ps} = h_{ps} (T_{ps} - T_{ps}^\infty)$ with temperature related via $\alpha^s T_{ps} = \alpha^e T_{ts}$, then the relationship

$\alpha^{\rho}(\rho^{-1}\bar{q})_{ps} \cdot \bar{n}_{ps} = \alpha^e g \beta^{-1}(\rho^{-1}\bar{q})_{ts} \cdot \bar{n}_{ts}$ gives rise to $\alpha^{\rho}(\rho^{-1}h)_{ps} = g\beta^{-1}\alpha^s(\rho^{-1}h)_{ts}$ with $\alpha^{sT^{\infty}}_{ps} = \alpha^e T^{\infty}_{ts}$. This latter relationship can sometimes introduce errors with the correction of an unrealistic external temperature T^{∞}_{ts}

5. Results and Discussion

It can be readily proved from a mathematical viewpoint that exact solutions of the stated problem always exist. This ensures that for any metal forming process, no matter how complicated, a theoretically exact model of it can be obtained in the scaled space. Indeed, the results of the computer modelling shown in Fig.1 illustrate the complete (within numerical simulation accuracy) similarity of two processes. These simulations were obtained for two artificial materials with scaled constitutive equations, corresponding speeds of the upper tools and with no heat exchange between the material and tools. It can be seen that under these conditions, all the characteristics of the metal flow (the shape of the flow lines, fields of strains, strain rates and temperatures) remain identical at all stages of the process. Complex geometry and non-monotonic and non-linear history of the thermomechanical conditions at different points in the material as well as the change in the direction of metal flow do not distort the accurate matching. This undoubtedly provides strong evidence for the correctness of the underpinning mathematical theory.

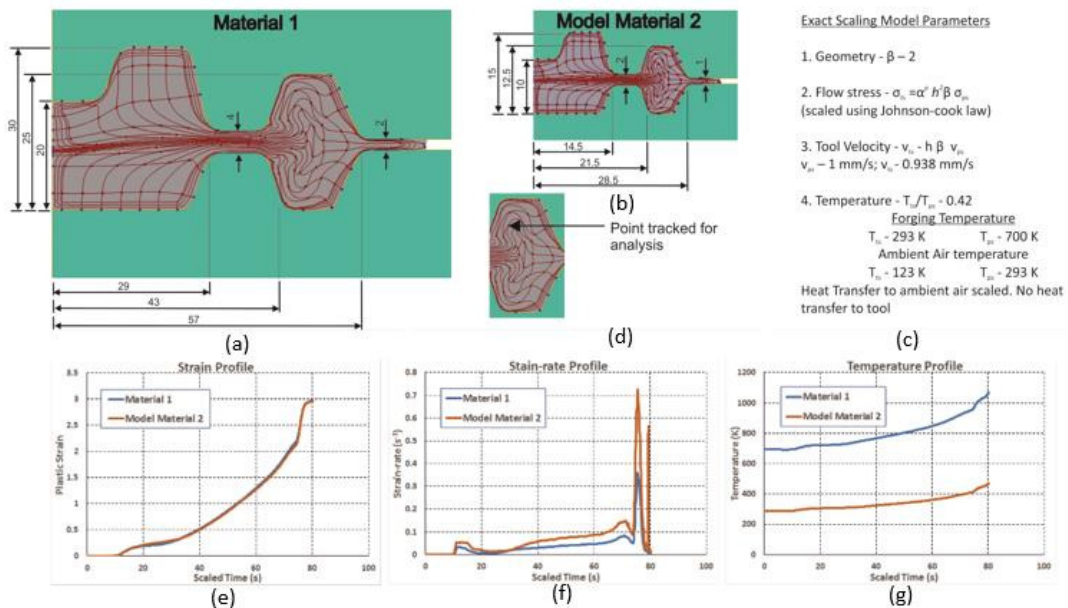


Fig. 1. Results of the FE simulation for two scaled disk forgings: geometry and flow lines for the (a) full-scale model (Material 1) and (b) scaled-down model (Model Material 2); (c) scaling parameters used in the models and (d) the point in the geometry tracked for detailed analysis; comparison of results from the simulation for Material 1 and Model material 2 – history of (e) strain, (f) strain-rate and (g) temperature.

However, the real interest in the scaling theory is related to the capability of its implementation for analysis and design of real technological processes. Hot-metal forging is an area of particular importance, where commonplace is the processing of small to (so-called) “large-scale” forgings (open or closed die), where the size of the part can be measured in dozens of meters and the weight in tons. Failures at these scales can be extremely costly and the design or optimization of any such process has to be proved to a high level of certitude. Of course, FE modelling provides a lot of support for understanding the mechanics of the metal flow, but for large complex parts involving multiple operations, analysis becomes computationally costly and “second opinion” is often required to crosscheck the reliability of the results.

Unfortunately, the exact scaling of real industrial process in a similar way to that was done with the artificial materials in the previous example is virtually impossible. The process itself dictates certain constraints, which cannot be adjusted. These constraints mainly come from the forging equipment and material properties. This situation is illustrated in Fig. 2. For example, the exact scaling demands all the temperatures in the scaled space to be proportional to the ones in the real process in the ratio $\alpha^{sT^{\infty}}_{ps} = \alpha^e T^{\infty}_{ts}$. Standard forging processes normally deal with three main temperatures: pre-heating temperature of the workpiece, temperature of the dies and the temperature of the ambient

air (additionally, during forging the workpiece heats up due to adiabatic heating). All of them have different ranges of variability. The temperature of pre-heating, depending on the material, can vary from 20 to 1200°C, dies (depending on the press) can be heated up to 300°C, ambient temperature is normally 20–30°C (industrial forging, due to cost restrictions, is mainly done in open air). This clearly shows that the ratio of temperatures obtained from the workpiece forging temperature hardly can be applicable to the boundary conditions. A similar situation exists with the speed of loading. For example, in the case of a screw press, only the energy of the blow can be scaled, but not the manner in which it is transferred to the workpiece. In the case of materials selection, three scaling requirements have to be satisfied at the same time for exact rheological similarity, i.e. $\gamma = \partial\bar{\sigma}/\partial\bar{\epsilon}$, $\zeta = \partial\bar{\sigma}/\partial\dot{\bar{\epsilon}}$ and $\xi = \partial\bar{\sigma}/\partial T$. The rheological behavior of the forging materials at elevated temperatures can be very complicated (due to different microstructural processes taking place in the material), so the best achievable solution will always be an approximate scaling over a limited range of temperatures and strain rates.

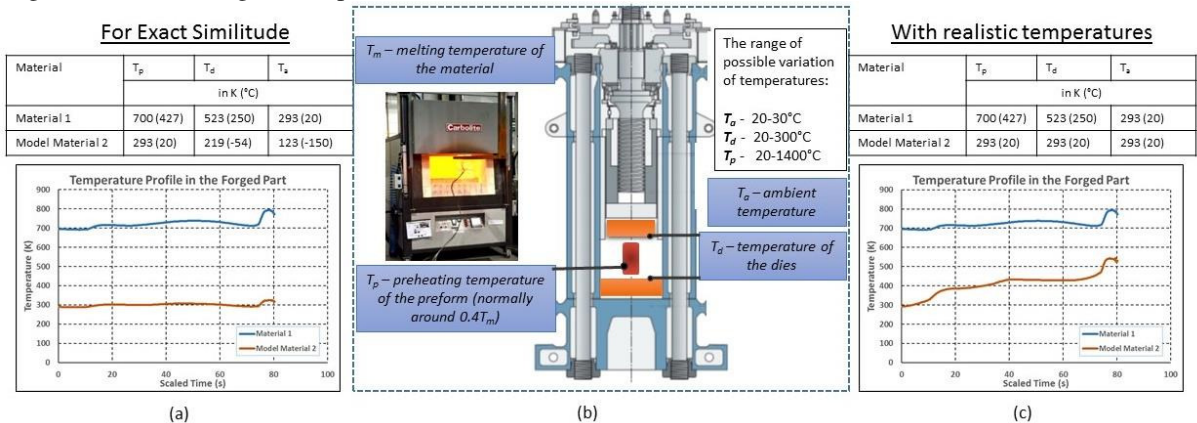


Fig 2. Illustration of constraints imposed on temperature - (a) Temperatures prescribed for the trial material to maintain exact similitude; (b) Constraints imposed on the temperatures under industrial forging conditions; (c) results of the compromise to meet the realistic temperature constraints.

This analysis of the situation brings us to the understanding that in the case of hot forging, physical modelling based on scaling reduces to the problem of finding practical solutions and assessing the cost of any compromises made. The inability to make exact-scaled modelling is one of the reasons why physical modelling, so popular in '50s and '60s [3-5], was later abandoned and almost forgotten. The absence of effective tools for data processing and computer modelling made the task of physical modelling extremely difficult being at best limited to a very narrow spectrum of outputs. With the advent of the new scaling theory, modern computational facilities and mathematical tools there is now an opportunity to halt this decline and breathe new life into the physical-modelling approach.

Acknowledgements

Acknowledgement and thanks are made to the EPSRC for financial support in the form of an EPSRC HVM Catapult Fellowship to enable Dr Davey to work at the Advanced Forming Research Centre (AFRC) in Glasgow UK.

References

- [1] J.T. Oden, S. Prudhomme, Estimation of modeling error in computational mechanics, *J. Comput. Phys.* 182(2) (2002) 496–515.
- [2] M.F. Ashby, Physical modelling of materials problems, *Mater. Sci. Tech. Ser.* 8 (1992) 102–111.
- [3] Green, A. P., The use of plasticine models to simulate the plastic flow of metals, *Phil. Mag.* 42 (1951) 365–373.
- [4] T. Altan, H. J. Henning, A. M. Sabroff, The use of model materials in predicting forming loads in metalworking, *J. Eng. Ind* 92(2) (1970) 444–451.
- [5] K.T. Chang, T.M. Brittain, An investigation of analog materials for the study of deformations in metal processing simulations, *J. Eng. Ind* 90(2) (1968) 381–386.
- [6] L.I. Sedov, Similarity and dimensional methods in mechanics, tenth ed., CRC Press, Florida, 1993.
- [7] O. Pawelski, Ways and limits of the theory of similarity in application to problems of physics and metal forming, *J. Mater. Process. Tech.* 34(1-4) (1992) 19–30.
- [8] K. Davey, R. Darvizeh, A. Al-Tamimi, Scaled Metal Forming Experiments: a Transport Equation Approach, Manuscript submitted for publication, *International Journal of Solids and Structures*, (2017).
- [9] K. Davey, R. Darvizeh, A. Al-Tamimi, Finite Similitude in Metal Forming, *MATEC Web of Conferences* 80(01005) (2016).